

# A study of coastal and harbor channel effects on Underwater Wireless Optical Communication systems with BCH and LDPC error correction codes

Lenin Joseph, and Sangeetha Anandan

**Abstract**—Owing to the benefits that they offer over traditional acoustic and RF communication, including higher data rates, reduced latency, and enhanced safety, underwater wireless optical communication (UWOC) systems have gained a solid focus. However, the transmission range is rather small compared with traditional radio frequency and acoustic communications because of turbulence which makes the light beam inside the water channel fade, absorb, and scatter. In this paper, a UWOC channel model mapped with LDPC and BCH error correction techniques is used to analyze the impulse response of the channel in coastal and harbor waters. The performance of the system based on its transmission length and bit error rate (BER) is evaluated. The link distance is determined to find the maximum link distance ensuring quality UWOC. The best performance has been observed with the 4-QAM-OFDM mapped channel with LDPC codes with maximum distance of 62 m in harbor water and 161.9 m in coastal water.

**Keywords**—Underwater communication; Bit Error rate; link distance

## I. INTRODUCTION

THE attention given to underwater wireless optical communication (UWOC) systems as an effective means of underwater communication is rapidly increasing and it has raised vital challenges for communication researchers. UWOC has versatile applications such as ocean monitoring, undersea expeditions, scientific marine exploration, voice and data communications between divers, investigations of climate change, mine reconnaissance, surveillance and disaster prevention [1]-[2] etc. Overall, UWOC is becoming more prevalent in marine ecosystems. As Optical carriers are the prime contributors to wired and wireless Internet of Underwater Things (IoUT) systems [3]-[4], the data rate requirement has been remarkably high [5].

However, wireless optical communication underwater faces extreme challenges. The underwater channel varies dynamically and therefore exhibits extreme challenges [6]. The optical properties of ocean water are affected by turbulence, absorption, and scattering phenomena. The impact of these factors causes amplitude and phase distortions and deflection of the optical path during beam propagation, thereby causing misalignment of the optical link. Thus, the bit error rate (BER) performance and signal-to-noise ratio (SNR) of a system using an optical signal as its primary carrier will be adversely affected.

Ocean water contains dissolved organic materials and other particles. When light energy is propagated through an underwater channel, the photons interact primarily with water molecules and the particles above. As a result, the photon's energy will be lost and this loss component is noted as the absorption coefficient, denoted by  $a(\lambda)$ . Similarly, interactions with particulate matter cause the photons to scatter away from their original propagation path. This phenomenon is denoted by the scattering coefficient  $b(\lambda)$  which causes optical beam to spread. Eventually, the beam is attenuated, inter-symbol interference (ISI) occurs and the BER performance is affected. The UWOC systems are thus limited to short ranges [7]-[12]. The total attenuation coefficient  $c(\lambda)$  can be written as the sum of the absorption coefficient  $a(\lambda)$  and scattering coefficient  $b(\lambda)$  as in Eq. (1).

$$c(\lambda)=a(\lambda)+b(\lambda) \quad (1)$$

Acoustic communication [13] underwater, though a suitable alternative, suffers from narrow bandwidth issues and multipath spreading. Besides, the data rate it offers is limited [14]-[15]. Radiofrequency (RF) communication; for underwater wireless channels can yield a high data rate; but only in short ranges. Recent developments in the RF communication field include the use of energy-efficient transceivers, compact equipment, also advancements in the design of antennas and suitable processing techniques [16].

The conductivity( $\sigma$ ), permittivity( $\epsilon$ ), permeability( $\mu$ ), and volume charge density( $\rho$ ) are critical in determining the speed of RF waves in underwater media. These factors; vary based on the environment and channel conditions. High-data-rate RF signals undergo more attenuation underwater than low-data-rate signals [17]. Due to these drawbacks of acoustic and RF communication methods, UWOC has received considerable attention because it can transmit high bit rate signals with lower latency than traditional methods. The resistance to electromagnetic interference is an added advantage for UWOC signals [18]. However, as we noted, one major concern of using UWOC is its short link distance. The research focus in UWOC is on two distinct viewpoints. Firstly, to increase performance, the link distance has to be improved. Subsequently, better performing short links are to be retained. Thus, possibility of merging collaborative and hybrid methodologies should be integrated and explored.

Authors are with VIT University, Vellore, India (e-mail: leninzmail@gmail.com, asangeetha@vit.ac.in ).



© The Author(s). This is an open-access article distributed under the terms of the Creative Commons Attribution License (CC BY 4.0, <https://creativecommons.org/licenses/by/4.0/>), which permits use, distribution, and reproduction in any medium, provided that the Article is properly cited.

## II. RELATED WORKS

The need for efficient technologies and aggregated research in the field of underwater wireless communication beyond acoustic communication is highlighted in the works of Guo, Y. et al. in 2022 [3]. In their work of Salman, M. et al. (2024), the challenges faced by UWOC which affects the large-scale deployments were indicated. The authors have presented a relay based UWOC system, which can enhance the link performance and expand the reception area of receivers [4].

Zhou et al. (2022), has demonstrated the underwater wireless optical communication system beyond 50 m distance. In their work, the authors have mathematically modeled the system, with the quantitative analysis of all the variables. The conclusion was that the water quality has a great impact on their experiment which essentially pointed out the research gap of analysing the quality of optical communication in relation to the types of water channels [5]. The factors like oceanic turbulence which significantly affects the performance of UWOC systems were discussed in the work of Sun, X. et al. (2020). The alignment losses and the energy efficiency issues were pointed out by the authors. Though the practical considerations were summarised, the authors conclude that the need for precise algorithms for randomly varying channel conditions is a major requirement for UWOC systems, particularly for future applications involving IoUT etc [11].

In 2023, Qu et al. reviewed the current trends and opportunities in using the underwater communication technologies like Acoustic, optical, and electromagnetic. The authors have mentioned some emerging technologies like magnetic, translational acoustic and RF and quantum communications. However, the limitations of optical communications in underwater, particularly the alignment problems, shortcomings in the long-distance transmissions were highlighted. The need for precise modelling based on techniques like deep learning were also addressed [15]. The channel models used for RF and optical methods for maritime communications were discussed in [16]. The authors have highlighted some research directions including visible light communication methods for onboard maritime applications. Jan, L. et al. (2023), have given research directions for implementing reliable communications systems in challenging environments. The authors have analysed the hybrid RF and UWOC in a multihop system [17]. All these works summarise the fact that the UWOC systems are sensitive to the harsh environment and turbulence. Also developing a suitable model which accounts for the dynamic environment is a major challenge. The selection of system model suitable for the water types and further mitigation of the issues with suitable channel coding is a task of prime importance.

## III. BACKGROUND

In this work, we analyze the performance of an optical link in an underwater channel, to functionally highlight the drawbacks of this approach to establish channel model that can account for the turbulent underwater environment and further establish short links and hybrid links using acoustic and optical counterparts. Thus, our focus is to simulate a channel impulse response function with the primary factors affecting the channel performance being the scattering coefficient, absorption coefficient and length of the channel.

### 3.1 Types of underwater channels

These primary categories of water which have been defined as clear ocean water, coastal water and harbor water that is turbid in nature are considered. In these different channels of water, the light beam attenuates differentially. The optical signals in pure seawater absorb due to its chemical composition, whereas a greater particle concentration in clear ocean water causes broad loss due to scattering. Compared to clear ocean water, coastal water has greater particle concentration which results in greater light beam scattering and absorption. In harbor water, the concentration of particles is at its maximum [19].

### 3.2 Factors of analysis and channel models

One might consider that UWOC is strongly affected by several environmental factors; therefore, any proposed model should consider turbulence a vital factor. As the range of a link increases, turbulence becomes more crucial, creating beam wandering and scintillation [20]. Several channel models use white noise as an additive in an underwater channel to observe BER with increased noise in the channel. However, these results do not account for varying channel lengths or absorption or scattering coefficients and are not ideal for performance analysis of the channel [21]. Channel models based on Inherent Optical Properties (IOP) and Radiative Transfer Theory (RTE) give promising solutions based on Monte Carlo numerical methods. IOP-based modeling schemes were reviewed as suitable for long-distance links especially in clear oceans. However, more computation time is required for complex problems [22].

#### 3.2.1 Double Gamma Function

Eq. (2) shows the Double Gamma Function (DGF) which was used to model the impulse response for UWOC in [23].

$$h(t) = C_1 t e^{-C_2 t} + C_3 t e^{-C_4 t} \quad (2)$$

This model which was inspired by Mooradian's work was used for modeling the impulse response in clouds. There are considerable differences in the case of ocean water channel modeling [23]–[26]. Thus, in [27], Li et al. concluded that the DGF model does not account for IOPs while finding the impulse response in UWOC channels.

#### 3.2.2 The combination of exponential and arbitrary power (CEAPF) function

The simulations we performed are based on [27], and use a function named CEAPF, which is combination of exponential and arbitrary power function. It is defined in Eq. (3). The Turbulence was kept separated from the overall attenuation to minimize the complexity of the analysis.

$$h(t) = C_1 \frac{(b\Delta L)^\alpha}{(b\Delta L + C_2')^\beta} \cdot e^{-a/b \cdot b\Delta L} \cdot e^{-a/b \cdot bL} \quad (3)$$

where  $\Delta L = v\Delta t$ ,  $C_1' = (bv)^\beta C_1$ , and  $C_2' = bvC_2$

$C_1$ ,  $C_2$ ,  $\beta$ , and  $\alpha$  are the four parameters to be found;  $a$  and  $b$  are already defined in the introduction section; and  $l$  is the length of the channel. This CEAPF given is a function of three real-world parameters namely, absorption( $a$ ), scattering coefficient( $b$ ), and length( $l$ ), of the channel, which strongly affects the channel's performance in real time.

#### IV. EXPERIMENTAL SETUP

##### 4.1 System model description

To conduct our experiments, we used Quadrature Amplitude Modulation(QAM)-with the Orthogonal Frequency Division Multiplexing (OFDM) mapped-Underwater Wireless Optical Communication (UWOC) channel for the analysis. The system model is explained as follows.

###### 4.1.1. Data rate

As our primary aim is to find the suitable link set up for enhancing the data rate, we assume that it depends on the factors like modulation scheme, error codes and signal quality.

###### 4.1.2 QAM

To transmit multiple bits per symbol, QAM technique is used to combine amplitude and phase variations. For higher data rates, we may use higher order QAM.

###### 4.1.3 OFDM and subcarriers

In our experiment, the OFDM is used as an enhancement scheme for data transmission efficiency. OFDM ensures that the high-speed data stream is divided into multiple subcarriers at a lower speed. These subcarriers are orthogonally spaced. Therefore, the chances of interference will be lowered, and reliability will be more especially in a dynamic underwater wireless channel.

Two different error correction codes were used in our experiment: the Low-Density Parity-Check (LDPC) and Bose-Chaudhuri-Hocquenghem (BCH) techniques. The use of these codes is to compensate for the undesirable effects from channel imperfections and to improve the BER performance.

###### 4.1.4 LDPC codes

LDPC codes are widely useful for wireless applications. As they are reliable, and are having near Shannon limit performance, they can be used in modern communication systems to utilize their efficient decoding capacity.

###### 4.1.5 BCH codes

They are most effective as powerful error correction codes especially when used in multiple bit error corrections within a block of data.

For an underwater channel in harbor and coastal waters, we transmit signals using OFDM with 4-QAM and 16-QAM with the error correction codes LDPC and BCH respectively. We analyze the bit error rate and the corresponding maximum distance the signal can travel from the received signal.

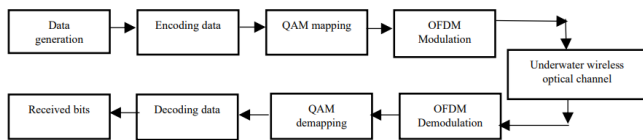


Fig. 1. Block diagram of QAM-OFDM mapped underwater wireless optical communication

##### 4.2 Design parameters

To transmit the generated OFDM signal to the simulated water channel, we convolve two functions namely, the channel

impulse function and the generated OFDM function. The data symbols modulate the orthogonally separated subcarriers. This method saves bandwidth and competes with multipath fading. The design parameters are shown in Table I. There are two kinds of channel impulses: the first is for the harbor water channel and the second is for the coastal water channel. The difference between these two water types is that they differ in their  $a(\lambda)$  and  $b(\lambda)$  values and in the constants of the equation. The values of  $a$  and  $b$  are relatively low for coastal water compared to those for harbor water.

TABLE I  
DESIGN PARAMETERS

Parameters	Values
Mapping and demapping Schemes	4-QAM, 16-QAM OFDM
Modulation type	OFDM
Number of subcarriers	52
Number of data bits	32400
Length of cyclic prefix	54
Error correction codes	BCH and LDPC encoding
Impulse response model	CEAPF model
Channel type	Harbor water and Coastal water
Absorption coefficient	$a=0.179 \text{ m}^{-1}$ (Coastal water) $a=0.366 \text{ m}^{-1}$ (Harbor water)
Scattering coefficient	$b=0.220 \text{ m}^{-1}$ (Coastal water) $b=1.829 \text{ m}^{-1}$ (Harbor water)
Speed of light	$2.237 \times 10^8 \text{ ms}^{-1}$

The design of the QAM-OFDM Mapped UWOC system used in our work is shown in Fig. 1. This system has been divided into three basic parts, i.e., transmitter, receiver, and channel [28]. Each of them is described in the following sections.

##### 4.3 Transmitting Section

Initially, the data for this experiment is generated. 32400 bits of data points are used. Following the generation of the data, error correcting techniques are used to encode the data.

The number of data points was doubled for LDPC encoding and tripled for BCH encoding after encoding. Furthermore, the encoded data were mapped to 4-QAM and 16-QAM. After mapping, OFDM was employed [29]-[30].

The bit vector that is transmitted is modified and subsequently passed on to a specific constellation at the transmitter side. The complex symbol stream that is generated is processed with the Inverse Fast Fourier Transform (IFFT).

Following IFFT, the output signal has a real value. Following the cyclic prefix (CP) extension, the subsequent operations performed include (i) parallel to serial conversion (ii) digital-to-analog conversion (DAC) and (iii) low-pass filtering (LPF) [31].

Additionally, we see that the quantity of information transferred can be maximized within the available bandwidth by mapping data to the QAM. The ability to select various QAM levels allows the system to be flexible under varying channel conditions and data rate demands. The QAM level can be selected to balance the data rate and stability in UWOC. When a higher-order QAM is used, the net bit rate decreases because a high SNR is needed to meet specific BER criteria, which means that certain subcarriers with lower SNR in the region of

high frequency must be ignored. Moreover, when a smaller electrical bandwidth is needed, a QAM with a higher order and larger spectral efficiency is adopted [32].

#### 4.4 Channel

As stated above, we simulated the water channel using CEAPF function [27]. The CEAPF parameters in coastal and harbor waters are summarised in Table II.

TABLE II  
CEAPF PARAMETERS IN COASTAL AND HARBOR WATERS [27]

Type	L(m)	FoV(°)	$C_1$	$C_2$	$\alpha$	$\beta$
On-axis harbor water	5.47	20	$5.244 \times 10^{-8}$	$5.02 \times 10^{-2}$	$-3.7 \times 10^{-2}$	3.019
		40	$7.937 \times 10^{-7}$	$2.96 \times 10^{-2}$	$-3.6 \times 10^{-2}$	1.793
		180	1.39	$2.331 \times 10^{-2}$	$-1.96 \times 10^{-2}$	1.564
	10.93	20	$1.677 \times 10^{-6}$	0.273	0.6577	3.169
		40	$1.320 \times 10^{-5}$	0.6657	0.4871	3.216
		180	$9.072 \times 10^{-6}$	0.4374	0.4798	2.005
	16.4	20	$2.168 \times 10^{-6}$	0.6994	1.569	3.739
		40	$3.207 \times 10^{-5}$	1.463	1.514	4.211
		180	$2.236 \times 10^{-5}$	1.818	1.255	3.039
On-axis, coastal water	45.45	20	$4.88 \times 10^{-7}$	0.4169	$-3.7 \times 10^{-2}$	3.019
		40	$5.525 \times 10^{-7}$	0.2458	$-3.6 \times 10^{-2}$	1.793
		180	$5.754 \times 10^{-7}$	0.1938	$-1.9 \times 10^{-2}$	1.564

Thus, in this CEAPF equation, we have the flexibility to input the values of these three parameters manually, which is the primary reason why we choose this equation for the impulse response and further analysis of the channel. However, the analysis is limited in terms of considering only the length variations in our work to simulate a channel function. This is because we focus on the maximum distance with which an optical link can effectively communicate with the minimum BER, in both harbor and coastal waters. For the rest of the parameters this paper followed the data described in [27]. Considering different receiver apertures via the channel impulse response method is found in our work as useful for accounting the temporal dispersion.

#### 4.5 Receiving Section

In the receiver, the received OFDM signal is demodulated after convolution with the channel. Further, QAM is demapped

and the signal is demodulated. After this stage, the data is decoded.

To determine the BER of the signal at the receiver, every bit received against every bit transmitted is compared. The error bits from the total bits are divided to arrive at the BER rate. For the next cycle, the length of the channel is increased, and the same process is repeated until the BER reaches the maximum value such that the received signal is no longer able to reach the length.

With this cycle, by increasing the length of the signal after each iteration, we can find the maximum distance a signal can travel in a particular channel. The simulations are carried out for both coastal and harbor waters for different combinations of error correction encoding techniques (i.e., LDPC or BCH) with 4-QAM and 16-QAM mappings. With this, we aim to find the best water channel to transmit longer distances and best combination of error correction and mapping schemes to ensure the maximum length with a low BER.

#### 4.6 Constraints, limitations and trade-offs

We considered primarily that, even though the real-time water channel impulse function is affected by absorption, scattering, and turbulence-induced fading as well as by the presence of particulate matter in the water, only the effects of absorption and scattering, such as IOPs of the underwater channel, were considered to reduce the analysis complexity.

The channel impulse function CEAPF [27] used in this work offers a channel response for only two different channel types, i.e., harbor water and coastal water. Moreover, there are limited data on the parameters (i.e.,  $C_1$ ,  $C_2$ ,  $\beta$ , and  $\alpha$ ) of Eq.3 used to simulate channels for other water types. Furthermore, we have plotted only three different fields of view (FoV) values, given as 180°, 40°, and 20° in our experiment study. The modulation was limited to the order of 16 because, with an increase in the modulation order, the data rate increases; thus, the signal attenuates massively even for short link lengths.

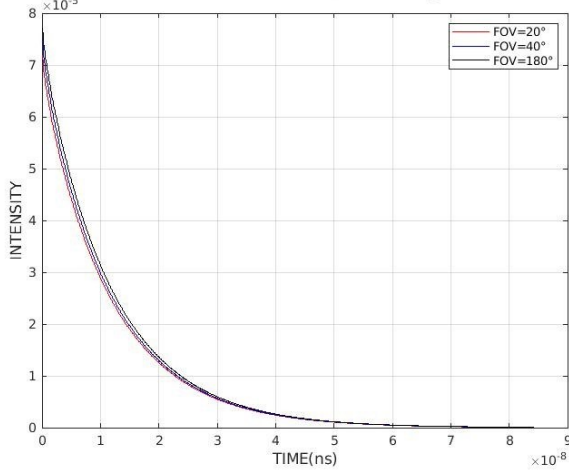
## V. RESULTS AND DISCUSSION

### 5.1 Impulse response of harbor water

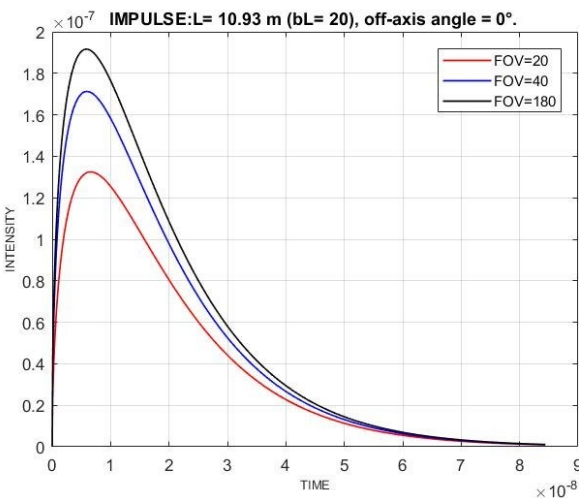
Fig. 3. shows the impulse response of the channel in harbor water for FoV values of 20°, 40° and 180°. The subparts are plotted for different link distances.

### 5.2 Impulse response of coastal water

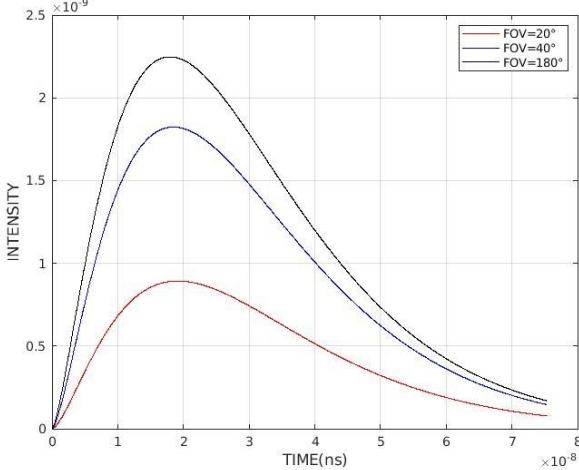
The impulse responses in the coastal water channel for FoV values of 20°, 40° and 180° are shown in Fig. 4. The plots are made for an off-axis angle of 0°. These plots verify that the effect of scattering is dominant when the link distance is extended. This is implied by the larger FoV values we obtain for long distances. The attenuation effect will increase for large distances; hence, there will be a reduction in the received power [27].

**IMPULSE RESPONSE:  $L = 5.47$  m ( $b(\lambda)L = 10$ ), off-axis angle =  $0^\circ$ : Harbour water**

(a)

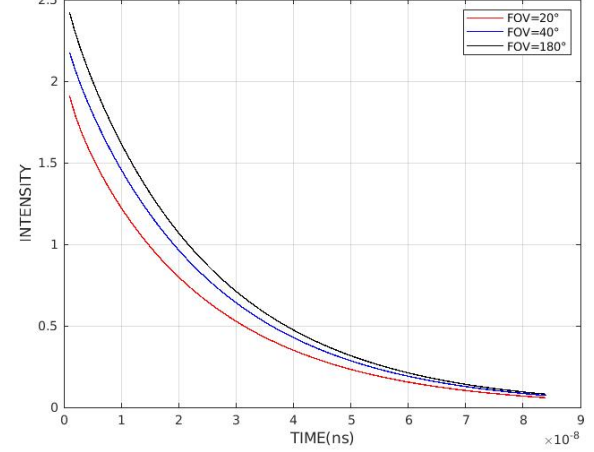


(b)

**IMPULSE RESPONSE FOR  $L = 16.40$  m ( $b(\lambda)L = 30$ ), off-axis angle =  $0^\circ$ : Harbour water**

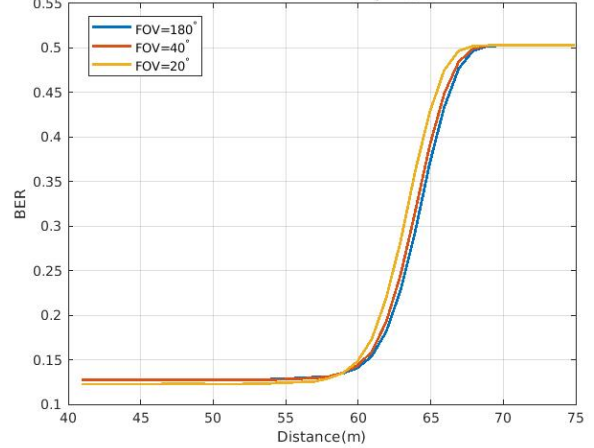
(c)

Fig.3. Impulse response of the channel in harbour water, with,

(a)  $L = 5.47$  m, (b)  $L = 10.93$  m, (c)  $L = 16.40$  m**Impulse response for coastal water  $L = 45.45$  ( $b(\lambda)L = 10$ )**Fig.4. Impulse response of the channel with  $L = 45.45$  m of coastal water

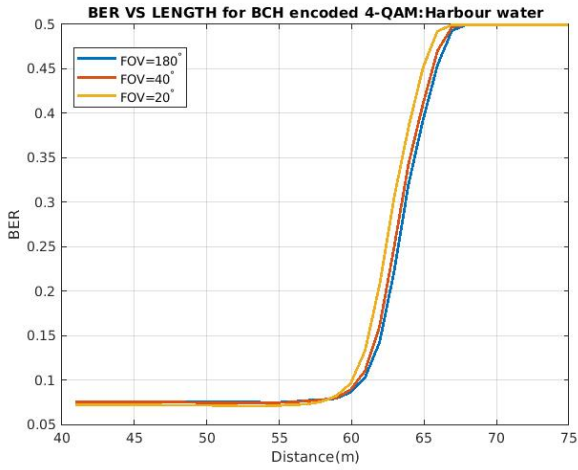
### 5.3 BER of harbor water

Fig. 5 shows the BER versus distance in meter plots with and without encoding in harbor waters. In Fig. 5 (a), QAM-OFDM modulation of order 4 is used without any encoding technique for FoV values of  $20^\circ$ ,  $40^\circ$  and  $180^\circ$ . The BER obtained is 0.1343, with a maximum distance of 62 m. In Fig. 5 (b), a fourth-order QAM-OFDM modulation technique is used with the BCH encoding technique. The BER recorded is 0.0717, with a maximum distance of 62 m. In Fig. 5 (c), the bit error rate is 0.1739, with a maximum distance of 62 m when the LDPC encoding technique is applied. In Fig. 5 (d), 5 (e) and 5 (f), QAM-OFDM modulation of order 16 is used without encoding, with BCH encoding and with LDPC encoding respectively, for the harbor water channel. The maximum distance in the first two cases is 62 m, with BER values of 0.3378 and 0.307. The bit error rate is 0.4919, with a maximum distance of 48 m in the last case.

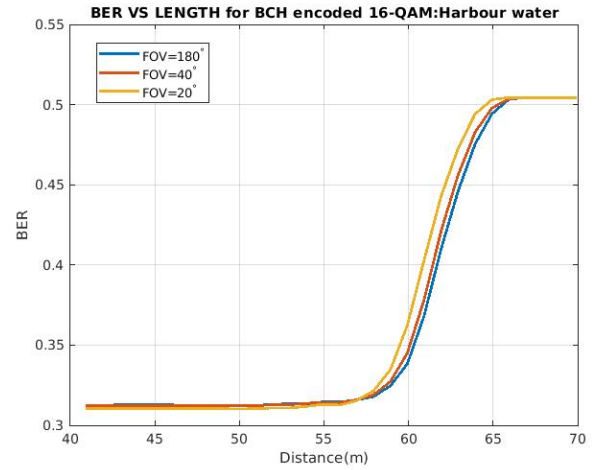
**BER VS LENGTH for without encoding 4-QAM:Harbour water**

(a)

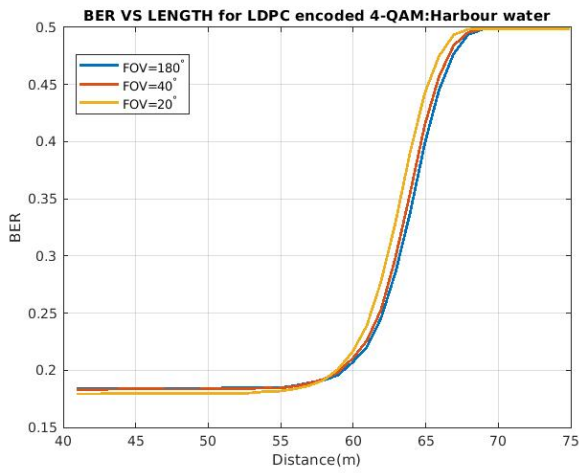




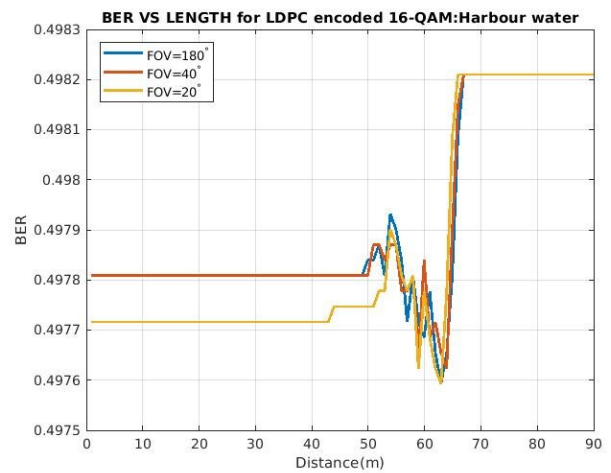
(b)



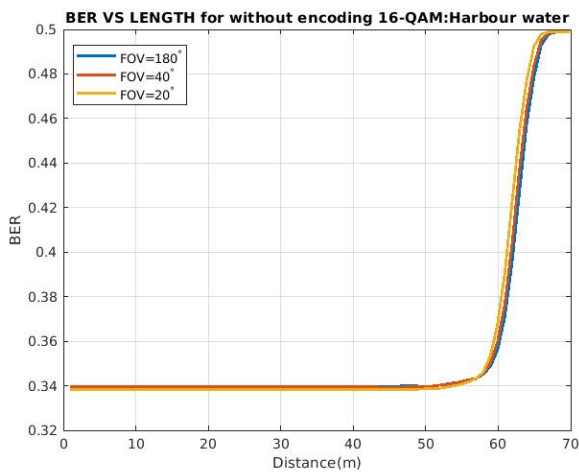
(e)



(c)



(f)



(d)

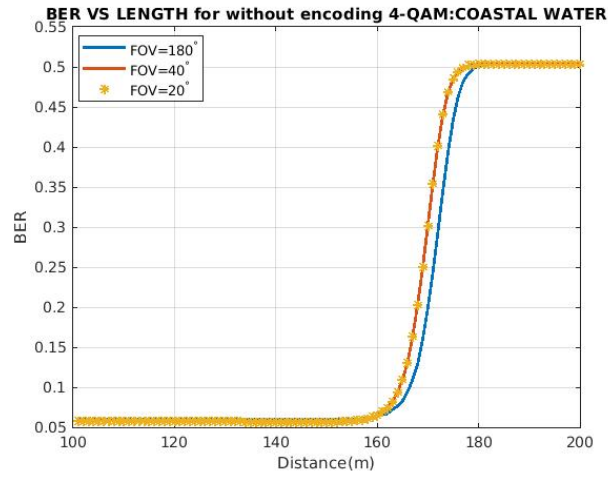
Fig.5 BER vs distance in harbor water

- (a) 4-QAM without encoding (b) 4-QAM with BCH encoding  
(c) 4-QAM with LDPC encoding (d) 16-QAM without encoding  
(e) 16-QAM with BCH encoding (f) 16-QAM with LDPC encoding

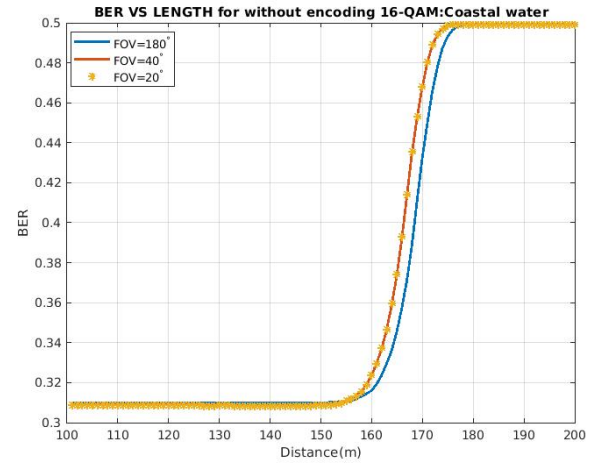
#### 5.4 BER of coastal water

The BER versus distance with and without encoding in coastal water are plotted in Fig. 6. In Fig. 6 (a), QAM-OFDM modulation of order 4 is used without any encoding technique with a BER value of 0.0601.

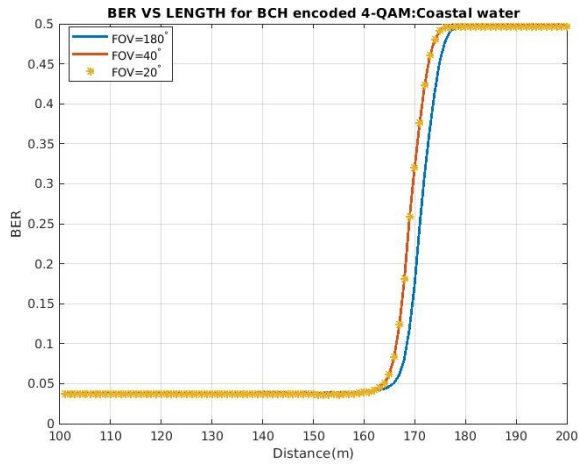
In Fig. 6 (b), the BER observed is 0.0525, with BCH encoding whereas in Fig 6 (c), the BER is 0.1260 with LDPC encoding. For all three of the above cases, the maximum link distance is 161.9 m. The graphs in Fig. 6 (d), (e) and (f) show similar plots with 16 QAM-OFDM in coastal water without encoding, with BCH encoding and with LDPC encoding respectively. The BERs observed are 0.3099, 0.2786 and 0.49858, with a maximum distance of 161.9 m in all three cases.



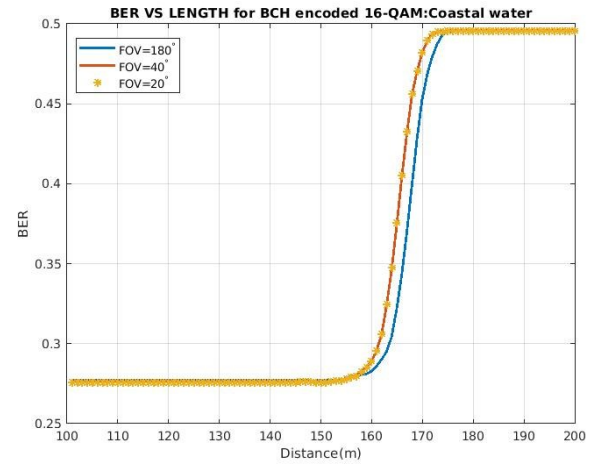
(a)



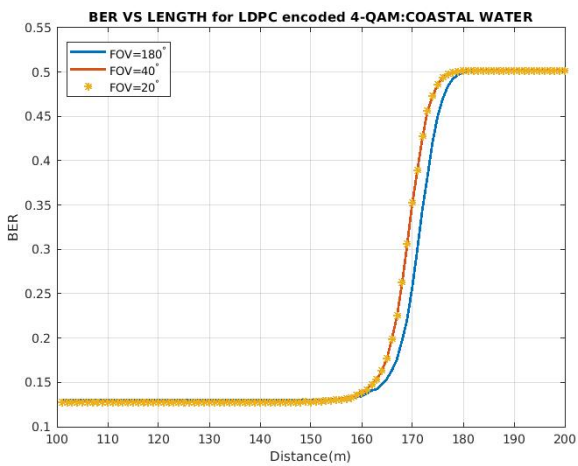
(d)



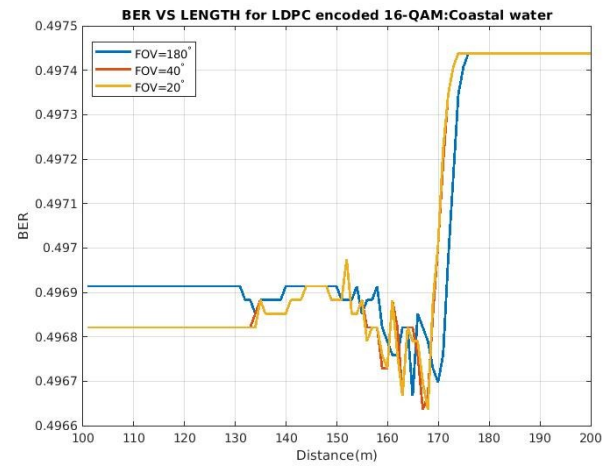
(b)



(e)



(c)



(f)

Fig.6. BER vs distance in coastal water

- (a) 4-QAM without encoding (b) 4-QAM with BCH encoding  
(c) 4-QAM with LDPC encoding (d) 16-QAM without encoding  
(e) 16-QAM with BCH encoding (f) 16-QAM with LDPC encoding

TABLE III  
BER AND DISTANCE IN HARBOR WATER

Sl.no	Modulation & order	Encoding	BER	Max. distance (m)
1	4-QAM-OFDM	BCH	$7.17 \times 10^{-2}$	62
2	4-QAM-OFDM	LDPC	$1.739 \times 10^{-1}$	62
3	16-QAM-OFDM	BCH	$3.07 \times 10^{-1}$	62
4	16-QAM-OFDM	LDPC	$4.919 \times 10^{-1}$	48

TABLE IV  
BER AND DISTANCE IN COASTAL WATER

Sl.no	Modulation & order	Encoding	BER	Max. distance (m)
1	4-QAM-OFDM	BCH	$5.25 \times 10^{-2}$	161.9
2	4-QAM-OFDM	LDPC	$1.26 \times 10^{-1}$	161.9
3	16-QAM-OFDM	BCH	$2.786 \times 10^{-1}$	161.9
4	16-QAM-OFDM	LDPC	$4.9858 \times 10^{-1}$	161.9

### 5.5 Summary of BER for various water channels

Table.3 summarizes the results obtained with two different encoding techniques in harbor channel. Table.4 summarizes that in coastal water channel. Our primary aim is to determine the maximum distance a signal can travel on an underwater channel, and to determine the minimum bit error rate (BER) that the channel offers. Another goal is to determine whether the encoding of the signal provides any lower BER to the channel. The results obtained are promising. However, not all encoding techniques provide a lower BER for the transmitting signal.

#### 5.5.1 Variation of BER with distance

Typically, we assume that, in a BER vs. distance graph, the BER rate gradually increases with respect to length and reaches the maximum BER. However, if we look at Fig. 4 and Fig. 5, we can observe that the BER remains constant and does not vary with length. However, after a certain point, the BER exponentially increases and reaches its maximum value. This observation is true for both coastal and harbor waters. This observation leads us to find the maximum transmission distance in our scenario.

#### 5.5.2 Variation of BER with encoding

According to the results table, the BER is relatively low for BCH-encoded signals compared to the nonencoded message signal for their respective counterparts. It has been observed that the BER is 22% lower for coastal water channels than for the harbor water for the same signal. Furthermore, we can also see that in the coastal channel, the message signal easily travels almost 61.4% more length than it travels in the harbor water of the QAM signal. One abnormal behavior we observe in the table is that the LDPC encoded signal offers a higher BER than the nonencoded signals and BCH-encoded signal. To justify this behavior, we have found that the LDPC code can be more effective if the SNR is more significant than 7 dB as in coastal

water channels, it is lower than 7 dB. Hence, we say that the LDPC-encoded signal results in a greater BER.

#### 5.5.3 Impact of temperature, salinity and turbulence on BER

Temperature and salinity have an impact on BER, which is highly variable. These two features vary inversely. Furthermore, maintaining the quality of communication for an underwater wireless optical link becomes challenging in the presence of turbulence [33]. In addition, when turbulence is within a particular range, boosting the transmission output may result in good BER performance. However, when the turbulence is high and strong, the power correction method is not effective [34].

#### 5.5.4 Requirement of high signal- to-noise ratio channel

As shown in [35], the OFDM technique performed without errors at 125 Mbit/s in pure water. For turbid waters, OFDM performs weaker. Even though OFDM could deliver a fast data rate on a static channel, it additionally requires a high SNR channel.

## VI. CONCLUSION AND FUTURE SCOPE

The viability of using higher-order QAM signals, which can be employed can be studied, when an electrical bandwidth is essential and when there is greater spectral efficiency. Multicarrier modulation schemes are promising solutions for enhancing system performance. As the underwater complex environment changes, system performance may improve with Spatial optical OFDM which is a hybrid OFDM technology [36].

Given that underwater optical channels are non-flat, non-stationary and dynamic, adaptive techniques should be used in conjunction with energy-efficient and economical solutions for future deployments to enhance link distance and performance. Vertical profile analysis is necessary for link establishment in deep water, as the link performance depends on the environment, particles and bubble sizes [37]-[38].

In our work, the underwater channel responses of coastal and harbor waters were modeled and evaluated. The maximum distance and BER performance for these channel types were further analyzed. Simulations clearly show that any signal transmitted in an underwater wireless channel suffers substantial attenuation. Also, it is evident that the water types significantly affect the distance and BER performance. In clear coastal waters, reduced scattering and absorption effects helps to achieve better system performance whereas in harbor and turbid waters, the signal undergoes significant degradation. Incorporation of different equalization techniques can enhance the performance of our system. Using these methods, the BER can be decreased by a significant number, and it is also possible to increase the link distance.[39]-[40]. Hybrid systems with integrated optical and other technologies are effective in mitigating the limitations thereby enhancing the reliable operation and operating range. Furthermore, the maximum distance of a hybrid communication system in different underwater channels should be evaluated combined with the best modulation schemes to obtain quality communication.



## REFERENCES

- [1] N. Saeed, A. Celik, T. Y. Al-Naffouri, and M. S. Alouini, "Underwater optical wireless communications, networking, and localization: A survey," *Ad Hoc Networks*, vol. 94, 2019, <https://doi.org/10.1016/j.adhoc.2019.101935>
- [2] Z. Zeng, S. Fu, H. Zhang, Y. Dong, and J. Cheng, "A Survey of Underwater Optical Wireless Communications," *IEEE Communications Surveys and Tutorials*, vol. 19, no. 1. Institute of Electrical and Electronics Engineers Inc., pp. 204–238, Jan. 01, 2017, <https://doi.org/10.1109/COMST.2016.2618841>
- [3] Y. Guo et al., "Current Trend in Optical Internet of Underwater Things," *IEEE Photonics J.*, vol. 14, no. 5, pp. 1–14, 2022, <https://doi.org/10.1109/JPHOT.2022.3195700>
- [4] M. Salman, J. Bolboli, R. P. Naik, and W. Y. Chung, "Aqua-Sense: Relay-Based Underwater Optical Wireless Communication for IoT Monitoring," *IEEE Open J. Commun. Soc.*, vol. 5, no. February, pp. 1358–1375, 2024, <https://doi.org/10.1109/OJCOMS.2024.3367457>
- [5] H. Zhou, M. Zhang, X. Wang, and X. Ren, "Design and Implementation of More Than 50m Real-Time Underwater Wireless Optical Communication System," *J. Light. Technol.*, vol. 40, no. 12, pp. 3654–3668, 2022, <https://doi.org/10.1109/JLT.2022.3153177>
- [6] J. Lloret, S. Sendra, M. Ardid, and J. J. P. C. Rodrigues, "Underwater wireless sensor communications in the 2.4 GHz ISM frequency band," *Sensors*, vol. 12, no. 4, pp. 4237–4264, Apr. 2012, <https://doi.org/10.3390/s120404237>
- [7] L. J. Johnson, "The Underwater Optical Channel," no. November, pp. 1–18, 2012, <https://doi.org/10.13140/RG.2.1.1295.7283>
- [8] J. W. Giles and I. N. Bankman, "Part 2 : Basic Design Considerations," *Appl. Phys.*, pp. 1–6.
- [9] A. Bricaud, M. Babin, A. Morel, and H. Claustre, "Variability in the chlorophyll-specific absorption coefficients of natural phytoplankton : Analysis and parameterization phytoplankton  $a \cdot h(A)$  was analyzed using a data set including 815 spectra determined chlorophyll concentration range ph values wer," *J. Geophys. Res.*, vol. 100, no. C7, pp. 13321–13332, 1995.
- [10] H. M. Oubei et al., "Light based underwater wireless communications," in *Japanese Journal of Applied Physics*, Aug. 2018, vol. 57, no. 8, <https://doi.org/10.7567/JJAP.57.08PA06>
- [11] [X. Sun et al., "A Review on Practical Considerations and Solutions in Underwater Wireless Optical Communication," *Journal of Lightwave Technology*, vol. 38, no. 2. Institute of Electrical and Electronics Engineers Inc., pp. 421–431, Jan. 15, 2020, <https://doi.org/10.1109/JLT.2019.2960131>
- [12] M. A. Khalighi, C. Gabriel, T. Hamza, S. Bourennane, P. Leon, and V. Rigaud, "Underwater wireless optical communication; Recent advances and remaining challenges," *Int. Conf. Transparent Opt. Networks*, pp. 2–5, 2014, <https://doi.org/10.1109/ICTON.2014.6876673>
- [13] H. P. Yoong, K. B. Yeo, K. T. K. Teo, and W. L. Wong, "Underwater wireless communication system: Acoustic channel modeling and carry frequency identification," *Int. J. Simul. Syst. Sci. Technol.*, vol. 13, no. 3 C, pp. 1–6, 2012, <https://doi.org/10.5013/ijsst.a.13.3c.01>
- [14] C. R. Berger, S. Zhou, J. C. Preisig, and P. Willett, "Sparse channel estimation for multicarrier underwater acoustic communication: From subspace methods to compressed sensing," *IEEE Trans. Signal Process.*, vol. 58, no. 3 PART 2, pp. 1708–1721, Mar. 2010, <https://doi.org/10.1109/TSP.2009.2038424>
- [15] Z. Qu and M. Lai, "A Review on Electromagnetic, Acoustic, and New Emerging Technologies for Submarine Communication," *IEEE Access*, vol. 12, no. December 2023, pp. 12110–12125, 2024, <https://doi.org/10.1109/ACCESS.2024.3353623>
- [16] F. S. Alqurashi, A. Trichili, N. Saeed, B. S. Ooi, and M. S. Alouini, "Maritime Communications: A Survey on Enabling Technologies, Opportunities, and Challenges," *IEEE Internet Things J.*, vol. 10, no. 4, pp. 3525–3547, 2023, <https://doi.org/10.1109/JIOT.2022.3219674>
- [17] L. Jan, G. Husnain, W. T. Sethi, I. U. Haq, Y. Y. Ghadi, and H. K. Alkahtani, "Empowering the Future of Hybrid MIMO-RF UOWC: Advanced Statistical Framework for Channel Modeling and Optimization for the Post-5G Era and beyond," *IEEE Access*, vol. 11, no. September, pp. 106361–106373, 2023, <https://doi.org/10.1109/ACCESS.2023.3314328>
- [18] K. Wang et al., "Evolution of Short-Range Optical Wireless Communications," *J. Light. Technol.*, vol. 41, no. 4, pp. 1019–1040, 2023, <https://doi.org/10.1109/JLT.2022.3215590>
- [19] M. F. Ali, D. N. K. Jayakody, and Y. Li, "Recent Trends in Underwater Visible Light Communication (UVLC) Systems," *IEEE Access*, vol. 10, pp. 22169–22225, 2022, <https://doi.org/10.1109/ACCESS.2022.3150093>
- [20] Z. Vali, A. Gholami, Z. Ghassemlooy, and D. G. Michelson, "System parameters effect on the turbulent underwater optical wireless communications link," *Optik (Stuttg.)*, vol. 198, Dec. 2019, <https://doi.org/10.1016/j.ijleo.2019.163153>
- [21] Y. Ata and K. Kiasaleh, "Analysis of Optical Wireless Communication Links in Turbulent Underwater Channels With Wide Range of Water Parameters," *IEEE Trans. Veh. Technol.*, vol. 72, no. 5, pp. 6363–6374, 2023, <https://doi.org/10.1109/TVT.2023.3235823>
- [22] L. Johnson, R. Green, and M. Leeson, "A survey of channel models for underwater optical wireless communication," *Proc. 2013 2nd Int. Work. Opt. Wirel. Commun. IWOW 2013*, pp. 1–5, 2013, <https://doi.org/10.1109/IWOW.2013.6777765>
- [23] S. Tang, Y. Dong, and X. Zhang, "Impulse response modeling for underwater wireless optical communication links," *IEEE Trans. Commun.*, vol. 62, no. 1, pp. 226–234, 2014, <https://doi.org/10.1109/TCOMM.2013.120713.130199>
- [24] H. Zhang and Y. Dong, "General Stochastic Channel Model and Performance Evaluation for Underwater Wireless Optical Links," in *IEEE Transactions on Wireless Communications*, Feb. 2016, vol. 15, no. 2, pp. 1162–1173, <https://doi.org/10.1109/TWC.2015.2485990>
- [25] J. Zhang, L. Kou, Y. Yang, F. He, and Z. Duan, "Monte-Carlo-based optical wireless underwater channel modeling with oceanic turbulence," *Opt. Commun.*, vol. 475, no. June, p. 126214, 2020, <https://doi.org/10.1016/j.optcom.2020.126214>
- [26] Y. Dong, H. Zhang, and X. Zhang, "On impulse response modeling for underwater wireless optical MIMO links," 2014 IEEE/CIC Int. Conf. Commun. China, ICC 2014, no. 2, pp. 151–155, 2015, <https://doi.org/10.1109/ICCChina.2014.7008262>
- [27] Y. Li, M. S. Leeson, and X. Li, "Impulse response modeling for underwater optical wireless channels," *Appl. Opt.*, vol. 57, no. 17, p. 4815, Jun. 2018, <https://doi.org/10.1364/ao.57.004815>
- [28] W. Cox and J. Muth, "Simulating channel losses in an underwater optical communication system," *J. Opt. Soc. Am. A*, vol. 31, no. 5, p. 920, May 2014, <https://doi.org/10.1364/josaa.31.000920>
- [29] C. T. Geldard, E. Guler, A. Hamilton, and W. O. Popoola, "An Empirical Comparison of Modulation Schemes in Turbulent Underwater Optical Wireless Communications," *J. Light. Technol.*, vol. 40, no. 7, pp. 2000–2007, 2022, <https://doi.org/10.1109/JLT.2021.3134090>
- [30] K. Nakamura, I. Mizukoshi, and M. Hanawa, "Optical wireless transmission of 405 nm, 145 Gbit/s optical IM/DD-OFDM signals through a 48 m underwater channel," *Opt. Express*, vol. 23, no. 2, p. 1558, 2015, <https://doi.org/10.1364/oe.23.001558>
- [31] H. Lu, M. Jiang, and J. Cheng, "Deep Learning Aided Robust Joint Channel Classification, Channel Estimation, and Signal Detection for Underwater Optical Communication," *IEEE Trans. Commun.*, vol. 69, no. 4, pp. 2290–2303, 2021, <https://doi.org/10.1109/TCOMM.2020.3046659>
- [32] J. Xu et al., "OFDM-based broadband underwater wireless optical communication system using a compact blue LED," *Opt. Commun.*, vol. 369, pp. 100–105, 2016, <https://doi.org/10.1016/j.optcom.2016.02.044>
- [33] Y. Ata, J. Yao, and O. Korotkova, "BER variation of an optical wireless communication system in underwater turbulent medium with any temperature and salinity concentration," *Opt. Commun.*, vol. 485, no. October 2020, p. 126751, 2021, <https://doi.org/10.1016/j.optcom.2021.126751>
- [34] R. Cai, M. Zhang, D. Dai, Y. Shi, and S. Gao, "Analysis of the underwater wireless optical communication channel based on a comprehensive multiparameter model," *Appl. Sci.*, vol. 11, no. 13, 2021, <https://doi.org/10.3390/app11136051>
- [35] Y. Guo et al., "Diffused-line-of-sight communication for mobile and fixed underwater nodes," *IEEE Photonics J.*, vol. 12, no. 6, 2020, <https://doi.org/10.1109/JPHOT.2020.3030544>
- [36] X. Huang, F. Yang, and J. Song, "Hybrid LD and LED-based underwater optical communication: state-of-the-art, opportunities, challenges, and trends [Invited]," *Chinese Opt. Lett.*, vol. 17, no. 10, p. 100002, 2019, <https://doi.org/10.3788/col201917.100002>

- [37] B. R. Angara, P. Shanmugam, and H. Ramachandran, "Underwater Wireless Optical Communication System Channel Modelling With Oceanic Bubbles and Water Constituents Under Different Wind Conditions," *IEEE Photonics J.*, vol. 15, no. 2, pp. 1–11, 2023, <https://doi.org/10.1109/JPHOT.2023.3258500>
- [38] Y. Lou, J. Cheng, D. Nie, and G. Qiao, "Performance of Vertical Underwater Wireless Optical Communications with Cascaded Layered Modeling," *IEEE Trans. Veh. Technol.*, vol. 71, no. 5, pp. 5651–5655, 2022, <https://doi.org/10.1109/TVT.2022.3156388>
- [39] H. Chen et al., "Toward Long-Distance Underwater Wireless Optical Communication Based on A High-Sensitivity Single Photon Avalanche Diode," *IEEE Photonics J.*, vol. 12, no. 3, Jun. 2020, <https://doi.org/10.1109/JPHOT.2020.2985205>
- [40] S. Jaruwatanadilok, "Channel Modeling and Performance Evaluation using Vector Radiative Transfer Theory," *IEEE J. Sel. Areas Commun.*, vol. 26, no. 9, pp. 1620–1627, 2008, [Online]. Available: <http://ieeexplore.ieee.org/xpl/articleDetails.jsp?arnumber=4686801>